GEOLOGY | THE GEOLOGICAL SOCIETY OF AMERICA®

https://doi.org/10.1130/G50687.1

Manuscript received 21 August 2022
Revised manuscript received 31 October 2022
Manuscript accepted 2 November 2022

Published online 20 January 2023

Slab window–related magmatism as a probe for pyroxenite heterogeneities in the upper mantle

Malcolm J. Hole[1], Sally A. Gibson[2] and Matthew C. Morris[2]
[1]Department of Geology and Geophysics, University of Aberdeen, Aberdeen AB24 3UE, UK
[2]Department of Earth Sciences, University of Cambridge, Cambridge CB2 3EQ, UK

ABSTRACT

New high-precision trace-element analyses of magmatic olivines point to a pyroxenite-dominated source for recent alkali basalts erupted above slab windows formed along the Antarctic Peninsula. Melting occurred at ambient mantle temperature, and basalts have geochemical compositions that are indistinguishable from ocean-island basalts (OIBs). We propose that the pyroxenite component originally resided in the upper mantle beneath the subducted slab; formation of a slab window allowed limited decompression and the generation of melts of garnet-pyroxenite, but little or no melting of mantle peridotite. The pyroxenite component in the mantle formed ca. 550 Ma, an age that does not require long-term recycling of subducting slabs to the core-mantle boundary. Enriched mid-ocean ridge basalt (E-MORB) from the adjacent extinct Phoenix Ridge owes its enriched trace-element compositions to mixing between small melt fractions of pyroxenite and peridotite during a period of decreased spreading rate prior to the death of the ridge ca. 3.3 Ma. It is likely that the variable trace-element enrichment seen in East Pacific Rise E-MORB distal from hotspots results from the same process of interactions between small-melt-fraction (<~5%) melts of pyroxenite and peridotite.

INTRODUCTION

Alkali basalts erupted above slab windows along continental margins may have ocean-island basalt (OIB)–like geochemical compositions; such lavas occur along the along the Pacific coast of North and Central America (Thorkelson et al., 2011) and along the Andean margin of South America (e.g., Søager et al., 2015). Basalts erupted at Seal Nunataks, Antarctic Peninsula (Fig. 1), are typical of this type of magmatism (e.g., Hole, 2021). The lavas are Ne- to Hy-normative alkali and transitional basalts (Fig. 2) with Mg# = 0.49–0.68, where Mg# = Mg/(Mg + Fe), and they are enriched in light rare earth elements (LREEs; $[La/Yb]_N$ = 5.3–13.5) and have Nb/Y > 0.6–2.4. They carry no vestige of a slab component, even though subduction was prolonged (>200 m.y.) prior to their eruption (Hole et al., 1991, 1993, 1994, 2021). By applying PRIMELT3 (Herzberg and Asimow, 2015) temperature modeling to melt inclusions from 5.6 to 3.3 Ma normal mid-ocean ridge basalt (N-MORB) from the nearby extinct Phoenix Ridge (Fig. 1; Hole, 2021), we constrained mantle potential temperature (T_P) along the Antarctic Peninsula to 1336 ± 30 °C, which is within the accepted range for ambient Pacific Ocean mantle (T_P = 1320–1350 °C; Herzberg and Asimow, 2015). However, LREE enrichment and high Nb/Y are generally considered to be features of melts generated from mantle peridotite when garnet is retained in the residue. The paradox here is that garnet is only stable on the dry peridotite solidus at T_P >1450 °C (e.g., Herzberg and Asimow, 2015), but, at this location, there is no evidence of the requisite temperature conditions for garnet-present melting of mantle peridotite.

OIB-like magmas are not restricted to the locus of slab windows along the Antarctic Peninsula (Fig. 1). In the past 4 m.y., OIB-like basalts were erupted: (1) above a slab window; (2) related to slab roll-back forming the James Ross Island Volcanic Group (Košler et al., 2009); and (3) at the northern end of the Bransfield Strait marginal basin (e.g., Spanish Rise; Fretzdorff et al., 2004). Also, the now-extinct Phoenix Ridge produced both normal (N) and enriched (E) MORB ($[La/Yb]_N$ and Nb/Y up to 6.5 and 1.5, respectively; Choe et al., 2007; Haase et al., 2011) before its demise at 3.3 Ma. Any petrogenetic model must therefore be able to explain this tectono-magmatic diversity.

Pyroxenite lithologies are widely accepted to be an intrinsic component of the upper mantle (e.g., Herzberg, 2011; Lambart et al., 2016). Garnet is stable on the pyroxenite solidus to lower pressures than peridotite (~1.9 GPa; Kogiso et al., 2003; Lambart et al., 2016), and at T_P of ~1320–1350 °C, pyroxenite may melt at higher pressures than peridotite (e.g., Lambart et al., 2016). It may be possible, therefore, to produce OIB-like basalts with LREE enrichment and high Nb/Y from a garnet pyroxenite source at ambient mantle temperatures.

To address the potential contribution of pyroxenite to recent basalts along the Antarctic Peninsula, we utilized new high-precision analyses of Ni, Ca, Zn, and Mn in magmatic olivines from lavas at Seal Nunataks because these minor elements are believed to be sensitive to lithological variations in the mantle and may be used to characterize pyroxenite melts (e.g., Howarth and Harris, 2017; Gleeson and Gibson, 2019).

OLIVINE CHEMISTRY INDICATIVE OF A PYROXENITE SOURCE

Olivines derived from crystallization of pyroxenite melts may have lower Ca and higher Ni contents than those derived from mantle peridotite at the same Fo content, where Fo = Mg/(Mg + Fe), and at T_P = 1350 °C (Figs. 3A and 3B; e.g., Herzberg, 2011). However, elevated Ni contents can also be a result of magma recharge and mixing of peridotite-derived melts (Gleeson and Gibson, 2019), and we cannot rule out such processes in contributing to the Ni content in Seal Nunataks olivine. Pyroxenite-derived lavas may exhibit lower whole-rock CaO for a given MgO compared to peridotite-derived magmas with the same MgO content and T_P. MORB typically contains ~12.3 wt% CaO at ~9.7 wt% MgO, whereas the Seal Nunataks

CITATION: Hole, M.J., Gibson, S.A., and Morris, M.C., 2023, Slab window–related magmatism as a probe for pyroxenite heterogeneities in the upper mantle: Geology, v. XX, p. , https://doi.org/10.1130/G50687.1

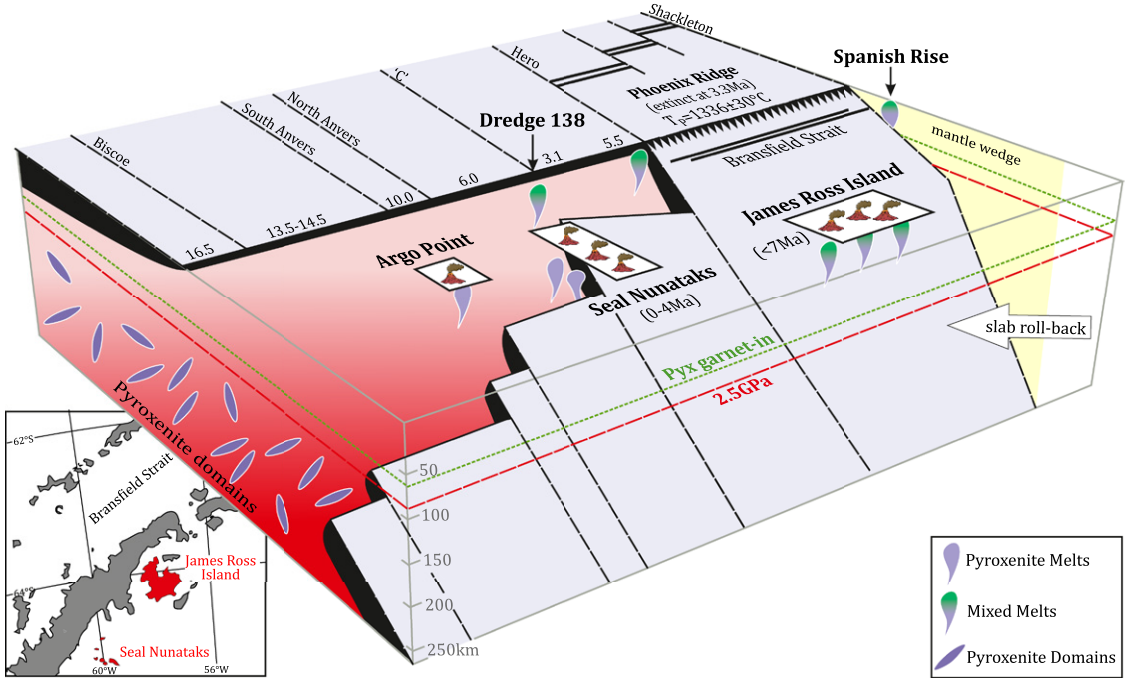

Figure 1. Sketch illustrating the development of the Antarctic Peninsula slab window, after Hole (2021). Numbers on each slab segment are the times of ridge-crest-trench collisions in Ma. Red and green dashed lines represent 2.5 GPa isobar when pyroxenite (Pyx) melting begins and the lower pressure limit for garnet stability, respectively. Triangle ornament represents active subduction; double lines represent spreading ridges. Volcano ornaments show locations of volcanic fields mentioned in the text. Inset at bottom left: Regional location.

lavas contain <9.0 wt% CaO at the same MgO content. Olivines that crystallize from pyroxenite-derived magmas have correspondingly low Ca contents (Fig. 3B), but the mineral-melt partition coefficient (K_d) for Ca in olivine decreases with increasing H_2O in the melt (Gavrilenko et al., 2016), such that low-Ca olivines may also crystallize from hydrous magmas. Importantly, the Seal Nunataks lavas carry no trace-element signature of a hydrous subduction component in their source, and we argue that the low-Ca olivines are a result of crystallization from a low-CaO pyroxenite-derived melt and not from a hydrous magma.

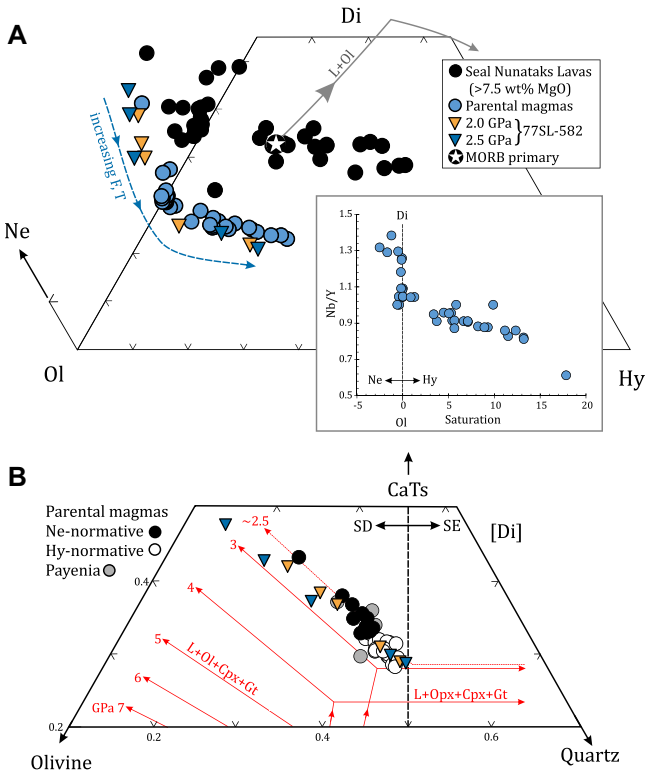

Figure 2. (A) CIPW normative tetrahedron for Seal Nunataks lavas with >7 wt% MgO (black dots) and their parental magmas (blue dots). For parental magma calculations, see the Supplemental Material (see footnote 1). Compositions of experimental melts of pyroxenite 77SL-582 are also shown (Keshav et al., 2004). Inset: Nb/Y versus index of silica saturation, expressed as Hy-normative (positive) or Ne-normative (negative) values. Average normal mid-ocean ridge basalt (N-MORB) is from Gale et al. (2013). Fractional crystallization trajectory is from Herzberg and Asimow (2015). N—nepheline; Hy—hypersthene; Ol—olivine; Di—diopside; F—melt fraction; *T*—temperature. (B) Projection from diopside onto plane of olivine–calcium Tschermak's molecule–quartz (Qz) for Seal Nunataks (Antarctica) parental pyroxenite-derived magmas, after Herzberg (2011). Red lines are cotectics with pressure indicated. Vertical dashed line separates silica-deficient (SD) and silica-enriched (SE) pyroxenite. Cpx—Clinopyroxene; Opx—orthopyroxene; Gt—garnet.

The transition elements Mn, Zn, and Fe are most sensitive to garnet-bearing residues during melting. Mineral-melt partition coefficients for Mn and Zn in garnet ($Kd_{Mn}^{Grt-melt}$~4.6 and $Kd_{Zn}^{Grt-melt}$~0.90; Le Roux et al., 2015) are such that high Zn/Mn is generated in partial melts of pyroxenite, leaving a garnet-bearing residue. Additionally, pyroxenite melts have higher Fe/Mn and Zn/Fe than peridotite melts because bulk partition coefficients (D) for Fe/Mn and Zn/Fe are lower in pyroxenite than in peridotite (Le Roux et al., 2015; Howarth and Harris, 2017). The lavas from Seal Nunataks contain olivines with Zn/Mn, Mn/Fe, and Zn/Fe values that are all indicative of melting of a pyroxenite source (Fig. 3C). They have similar Zn/Fe and Mn/Fe values to the well-documented pyroxenite-derived Mwenzi picrites from the Karoo flood basalt province (Howarth and Harris, 2017) and the most extreme compositions of olivine in the global database, which are from Orkhon, Mongolia (Zhang et al., 2021). Andean margin lavas (Payenia basalts, Argentina; Søager et al., 2015) straddle the pyroxenite-peridotite boundary in Figure 3C, suggesting a mixed pyroxenite-peridotite origin.

Pyroxenite-Derived Parental Magmas

Major elements show that the Seal Nunataks lavas have crystallized only olivine (Hole, 2021), and therefore basalts containing >7.5 wt% MgO were used to estimate the composition of their parental magmas by incrementally adding equilibrium olivine to whole-rock compositions using the method of Herzberg (2011). The pressure-dependent CMAS ($CaO-MgO-Al_2O_3-SiO_2$) projection (Herzberg, 2011) indicates that

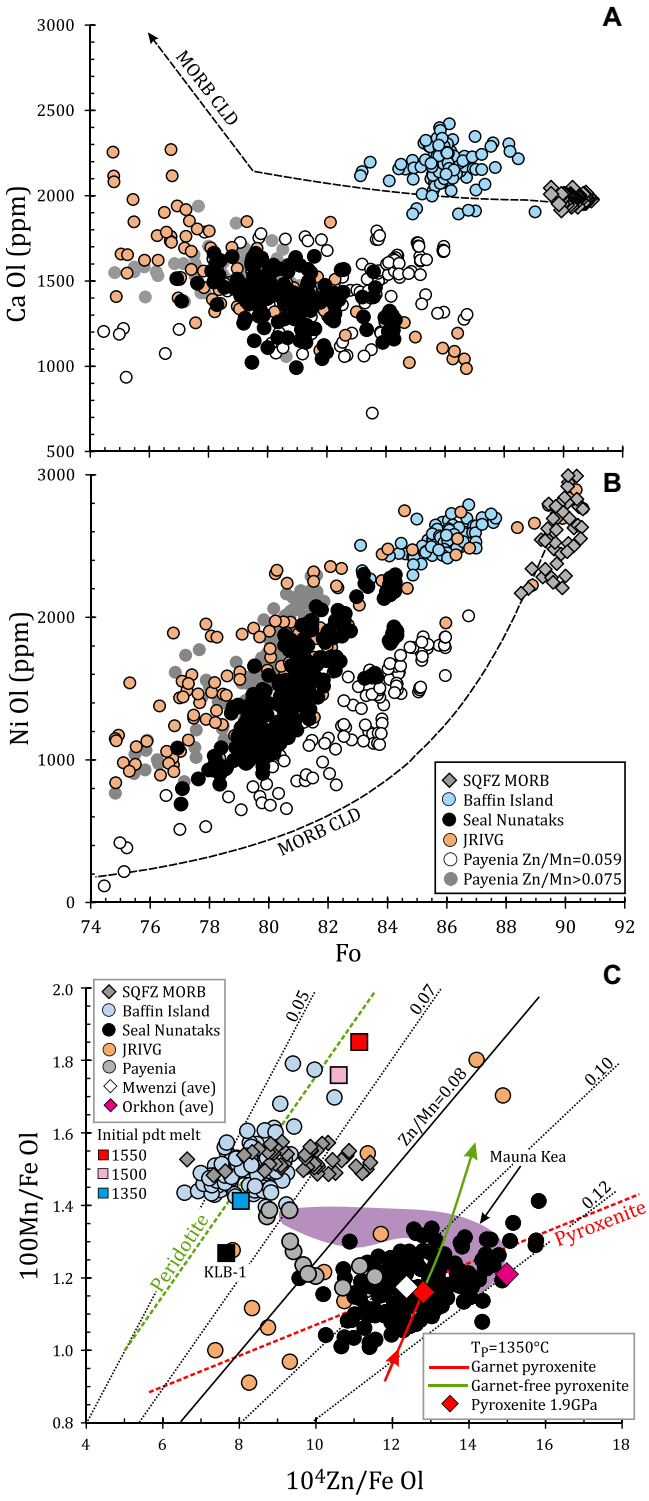

Figure 3. (A) Ca (ppm) and (B) Ni (ppm) versus Fo content of olivines (Ol), where Fo = Mg/(Mg + Fe). Mid-ocean ridge basalt (MORB) crystal lines of descent (CLD) were calculated using PRIMELT3 (Herzberg and Asimow, 2015). Seal Nunataks (Antarctica) Ca data were analyzed by laser ablation–inductively coupled plasma–mass spectrometry (LA-ICP-MS), and Ni was analyzed by electron microprobe analysis (EMPA). Payenia (Argentina) olivines are subdivided based on Zn/Mn. (C) 100Mn/Fe versus 10^4 Zn/Fe in magmatic olivines (Ol). Trends for olivine in equilibrium with peridotite- and pyroxenite-derived magmas (green and red dashed lines, respectively) are from Howarth and Harris (2017). Melting pathways for garnet and garnet-free pyroxenite are based on the parental melt for sample R.3717.1. Red diamond is the composition at transition from garnet to garnet-absent melting (1.9 GPa). Black lines are contours of Zn/Mn. Compositions of initial melts of peridotite (pdt) at T_P = 1350, 1500, and 1550 °C are based on modeled primary magmas of peridotite at those temperatures from Hole and Millett (2016). Data sources: Seal Nunataks—this study; Payenia—Søager et al. (2015); JRIVG (James Ross Island Volcanic Group)—Altunkaynak et al. (2019); Baffin Island, Siqueiros Fracture Zone (SQFZ), MORB, and peridotite KLB-1—Putirka et al. (2018).

melting occurred at ≤2.5 GPa, and in Figure 2, parental melts fall close to the compositions of experimental melts of a silica-deficient pyroxenite (sample 77SL-5822) at 2.0 and 2.5 GPa (Keshav et al., 2004). Additionally, Nb/Y exhibits a negative covariation with silica saturation (Fig. 2), suggesting that the two parameters are related by extent of melting, consistent with the results of the melting experiments of Keshav et al. (2004).

PERIDOTITE AND PYROXENITE MELTING

We investigated the melting conditions for mantle comprising 80% peridotite and 20% pyroxenite (Lambart, 2017) using Melt-Px (Lambart et al., 2016) for a silica-deficient pyroxenite composition (sample 77SL-582) at T_P = 1350 °C. We assumed a rutile-free modal composition of 80% clinopyroxene and 20% garnet, with garnet being stable on the pyroxenite solidus to ≥1.9 GPa (e.g., Pertermann et al., 2004). Below 1.9 GPa, we assumed the pyroxenite contained both clinopyroxene and orthopyroxene. There is little difference in the initial pressure of melting (P_i) of 77SL-582 (P_i^{pyx} = 2.3 GPa) and peridotite (P_i^{pdt} = 2.2 GPa), and this estimate of P_i^{pyx} is close to the independently obtained value ≤2.5 GPa from the CMAS projection. The differing melt productivity rates for pyroxenite and peridotite require that ~13% melting of garnet-pyroxenite could be achieved over the pressure interval 2.4–1.9 GPa, but only <3% melting of spinel-peridotite would occur; i.e., any melt produced in this pressure interval would be predominantly generated from garnet-pyroxenite (see the Supplemental Material[1]).

We used the composition of calculated accumulated fractional melts of pyroxenite and peridotite (see the Supplemental Material) to investigate covariations between Nb/Y and $[Tb/Yb]_N$ in basaltic magmas (Fig. 4). These ratios are of interest because $D_{Nb} \rightarrow 0$ during melting of any rutile-free mantle lithology, and Nb/Y exhibits the greatest variability in the data. Garnet-bearing residues may be identified using $[Tb/Yb]_N$ since $Kd_{Yb}^{Grt-melt} >> Kd_{Tb}^{Grt-melt}$ (e.g., Pertermann et al., 2004). Figure 4 shows that garnet-pyroxenite melts have $[Tb/Yb]_N$ in the range 2.7–3.5 and Nb/Y > 1, while garnet-free pyroxenite melts exhibit a progressive decrease in $[Tb/Yb]_N$ and Nb/Y toward the composition of N-MORB with increasing melting. Isobaric mixing of peridotite and pyroxenite melts will begin at ~2.2 GPa, and, in Figure 4, the Seal Nunataks data occupy the region for pure pyroxenite melts or isobaric mixed melts at ~1.8–2.2 GPa. The melting trajectories for Zn, Fe, and Mn based on olivine in equilibrium with major elements and the trace-element compositions computed from the accumulated fractional melt model are shown in Figure 3. The 1.9 GPa melt model falls within the Seal Nunataks data array and demonstrates that the proposed melting model is internally consistent for the rare earth elements, Nb, Y, Zn, Mn, and major elements.

A second trend of low $[Tb/Yb]_N$ values in Figure 4 is shown by Phoenix Ridge MORB, trench-proximal OIB-like lavas at Dredge site 138 (Hole and Larter, 1993), and some James Ross Island Volcanic Group lavas (Figs. 1 and 3). These lavas have $[Tb/Yb]_N < 1.5$ but Nb/Y = 0.05–2.0, and they fall close to the calculated mixing line between small melt fractions of pyroxenite and first-formed melts of peridotite. The variable Nb/Y values along this trend

[1]Supplemental Material. Details of accumulated fractional melting model, partition coefficients and analytical techniques employed during the study. Please visit https://doi.org/10.1130/10.1130/GEOL.S.21824805 to access the supplemental material and contact editing@geosociety.org with any questions.

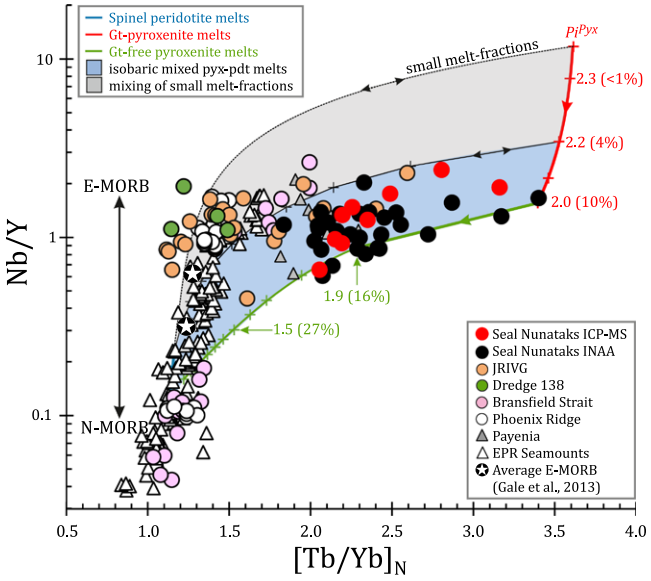

Figure 4. Nb/Y versus [Tb/Yb]$_N$ for Antarctic Peninsula lavas. In this model, peridotite would begin to melt at 2.2 GPa. Blue shaded region represents the locus of all melts formed by isobaric melting of pyroxenite (pyx) and peridotite (pdt). Gray area represents the locus of all melts that might form by interaction between small melt fractions of pyroxenite and first formed melts of peridotite. Red and green lines represent the locus of "pure" garnet (Gt) pyroxenite and garnet-free pyroxenite, respectively, with pressure in GPa and percent melting indicated. E-/N-MORB—enriched/normal mid-ocean ridge basalt; EPR—East Pacific Rise; ICP-MS—inductively coupled plasma–mass spectrometry; INAA—instrumental neutron activation analysis. Data sources: Bransfield Strait—Fretzdorff et al. (2004); Seal Nunataks—this study, and Hole (1990); JRIVG (James Ross Island Volcanic Group)—Hole et al. (1993) and Kosler et al. (2009); Dredge 138—Hole and Larter (1993); Phoenix MORB—Choe et al. (2007) and Hasse et al. (2011); Payenia (Argentina)—Søager et al. (2015).

cannot be attributed solely to garnet-pyroxenite melting because the [Tb/Yb]$_N$ of the basalts does not indicate a garnet-bearing source. While $D_{Nb} < D_{Tb}$ during melting of peridotite, this difference in D would not be sufficient to generate, on its own, the N-MORB and E-MORB trend shown in Figure 4. In addition, Phoenix Ridge E-MORB and N-MORB are isotopically distinct (Choi et al., 2013; Haase et al., 2011), which does not support an origin by variable melting from a single source.

The mixing of small melt fractions can only be achieved under specific mantle conditions. For silica-depleted pyroxenite, $P_i^{pyx}/P_i^{pdt} < 1.5$ GPa, but for most silica-enriched pyroxenite, $P_i^{pyx}/P_i^{pdt} > 1.5$ GPa (e.g., G2; $P_i^{pyx}/P_i^{pdt} \sim 2.8$ GPa), variations which are independent of T_P (see the Supplemental Material). For a silica-enriched pyroxenite-peridotite assemblage with P_i^{pyx}/P_i^{pdt} of ~2 GPa, an ~30% pyroxenite melt with [Tb/Yb]$_N$ of ~1.5 and Nb/Y of ~0.3 would be generated before peridotite began to melt. However, this melt would have the major-element composition of dacite (Pertermann et al., 2004), an unlikely candidate for the origin of E-MORB.

Significantly, depleted mantle (DM) Nd model ages for Seal Nunatak lavas (T_{DM} = 580–220 Ma; Hole, 1990; Hole et al., 1993) and Phoenix Ridge E-MORB (T_{DM} ~425 Ma) do not require the pyroxenite source to be ancient and point to an origin that does not require long-term (~2 b.y.) recycling of subducted slabs to the core-mantle boundary, followed by their re-emergence in the upper mantle via plume ascent or deep-seated mantle convection.

Slab Removal and Decompression Melting

The above arguments require "young" pyroxenite to reside in the upper mantle beneath the subducted slab. This in turn provides an explanation for the lack of any subduction signature in the recent Antarctic Peninsula basalts. We envisage a "marble-cake" or "plum pudding" mantle (Allègre and Turcotte, 1986; Carlson, 1988), where the pyroxenite component is possibly derived by delamination of subcontinental lithospheric mantle (e.g., Thorkelson and Breitsprecher, 2005; Sheldrick et al., 2020).

For the Seal Nunataks slab-window basalts, we estimate that the age of the oceanic lithosphere at 100 km depth was at least 15–20 Ma at the time of ridge-crest-trench collision, corresponding to a lithospheric thickness of ~40 km (Hole and Larter, 1993). Formation of a slab window would allow decompression equivalent to the vertical thickness of the thermal slab. Assuming a slab dip of ~20°, ~46 km of decompression could occur (~1.4 GPa). The depth to the top of the slab at 200 km from the trench would be ~70 km or ~2.3 GPa. The creation of a slab window would therefore allow decompression of mantle from ~4.0 GPa to ~2.3 GPa. This would be sufficient to generate garnet-pyroxenite melts at T_P = 1350 °C but would not allow peridotite melting. A steeper slab dip could prevent any magmatism, whereas a shallower dip, or a location closer to the trench, might promote more melting of peridotite. This is an encouraging explanation for the localized nature of occurrences of alkali basalts along continental margins. Where slab roll-back occurred (e.g., James Ross Island Volcanic Group), the added dynamic of lateral movement of mantle may have caused more extensive melting of peridotite and widespread magmatism. Indeed, we concur with Thorkelson and Breitsprecher (2005), who theorized that lateral mantle flow around slab windows is significant and might shift pyroxenite to a variety of locations within the arc–back-arc system.

At the Phoenix Ridge, decreasing spreading rate prevented large-scale decompression melting of peridotite and allowed the signature of mixed small melt fractions (<~5%) to become prevalent. We suggest that mixing of small melt fractions of pyroxenite with peridotite sourced from the upper mantle is a viable explanation for trace-element heterogeneities observed in off-axis seamounts and ridges (e.g., East Pacific Rise; Fig. 4), as described by Anderson et al. (2020).

ACKNOWLEDGMENTS

We are grateful to Rob Clarke for making the thin sections, and Iris Buisman and Jason Day for assistance with the electron microprobe and laser ablation–inductively coupled plasma–mass spectrometry. The manuscript was improved by the comments of Derek Thorkelson and an anonymous reviewer.

REFERENCES CITED

Allègre, C.J., and Turcotte, D.L., 1986, Implications of a two-component marble-cake mantle: Nature, v. 323, p. 123–127, https://doi.org/10.1038/323123a0.

Altunkaynak, S., Unal, A., Howarth, G.H., Aldanmaz, E., and Nyvlt, D., 2019, The origin of low-Ca olivine from ultramafic xenoliths and host basaltic lavas in a back-arc setting, James Ross Island, Antarctic Peninsula: Lithos, v. 342–343, p. 276–287, https://doi.org/10.1016/j.lithos.2019.05.039.

Anderson, M., Wanless, V.D., Perfit, M., Conrad, E., Gregg, P., Fornari, D., and Ridley, W.I., 2020, Extreme heterogeneity in mid-ocean ridge mantle revealed in lavas from the 8°20′N near-axis seamount chain: Geochemistry, Geophysics, Geosystems, v. 22, https://doi.org/10.1029/2020GC009322

Carlson, R.W., 1988, Layer cake or plum pudding?: Nature, v. 334, p. 380–381, https://doi.org/10.1038/334380a0.

Choe, W.-H., Lee, J.-I., Lee, M.-J., Hur, S.-D., and Jin, Y.-K., 2007, Origin of E-MORB in a fossil spreading center: The Antarctic-Phoenix Ridge, Drake Passage, Antarctica: Geosciences Journal, v. 11, p. 185–199, https://doi.org/10.1007/BF02913932.

Choi, S.-H., Schiano, P., Chen, Y., Devidal, J.-L., Choo, M.-K., and Lee, J.-I., 2013, Melt inclusions in olivine and plagioclase phenocrysts from Antarctic–Phoenix Ridge basalts: Implications for origins of N- and E-type MORB parent magmas: Journal of Volcanology and Geothermal Research, v. 253, p. 75–86, https://doi.org/10.1016/j.jvolgeores.2012.12.008.

Fretzdorff, S., Worthington, T.J., Hasse, K.M., Hekinian, R., Franz, L., Keller, R., and Stoffers, P., 2004, Magmatism in the Bransfield Basin: Rifting of the South Shetland arc?: Journal of Geophysical Research, v. 109, B12208, https://doi.org/10.1029/2004JB003046.

Gale, A., Dalton, C.A., Langmuir, C.H., Su, Y., and Shilling, J.-G., 2013, The mean composition of ocean ridge basalts: Geochemistry, Geophysics,

Geosystems, v. 14, p. 489–518, https://doi.org/10.1029/2012GC004334.

Gavrilenko, M., Herzberg, C., Vidito, C., Carr, M.J., Tenner, T., and Ozerov, A., 2016, A calcium-olivine hygrometer and its application to subduction zone magmatism: Journal of Petrology, v. 57, p. 1811–1832, https://doi.org/10.1093/petrology/egw062.

Gleeson, M.L.M., and Gibson, S.A., 2019, Crustal controls on apparent mantle pyroxenite signals in ocean-island basalts: Geology, v. 47, p. 321–324, https://doi.org/10.1130/G45759.1.

Haase, K.M., Beier, C., Fretzdorff, S., Lest, P.T., Livermore, R.A., Barry, T.L., Pearce, J.A., and Hauff, F., 2011, Magmatic evolution of a dying spreading axis: Evidence for the interaction of tectonics and mantle heterogeneity from the fossil Phoenix Ridge, Drake Passage: Chemical Geology, v. 280, p. 115–125, https://doi.org/10.1016/j.chemgeo.2010.11.002.

Herzberg, C., 2011, Identification of source lithology in the Hawaiian and Canary Islands: Implications for origins: Journal of Petrology, v. 52, p. 113–146, https://doi.org/10.1093/petrology/egq075.

Herzberg, C., and Asimow, P.D., 2015, PRIMELT3 MEGA.XLSM software for primary magma calculation: Peridotite primary magma MgO contents from the liquidus to the solidus: Geochemistry, Geophysics, Geosystems, v. 16, p. 563–578, https://doi.org/10.1002/2014GC005631.

Hole, M.J., 1990, Geochemical evolution of Pliocene–Recent post-subduction alkalic basalts from Seal Nunataks, Antarctic Peninsula: Journal of Volcanology and Geothermal Research, v. 40, p. 149–167, https://doi.org/10.1016/0377-0273(90)90118-Y.

Hole, M.J., 2021, Antarctic Peninsula: Petrology, *in* Smellie, J.L., et al., eds., Volcanism in Antarctica: 200 Million Years of Subduction, Rifting and Continental Break-Up: Geological Society, London, Memoir 55, p. 327–343, https://doi.org/10.1144/M55-2018-40.

Hole, M.J., and Larter, R.D., 1993, Trench-proximal volcanism following ridge crest-trench collision along the Antarctic Peninsula: Tectonics, v. 12, p. 897–910, https://doi.org/10.1029/93TC00669.

Hole, M.J., and Millett, J.M., 2016, Controls of mantle potential temperature and lithospheric thickness on magmatism in the North Atlantic igneous province: Journal of Petrology, v. 57, p. 417–436, https://doi.org/10.1093/petrology/egw014.

Hole, M.J., Rogers, G., Saunders, A.D., and Storey, M., 1991, Relation between alkalic volcanism and slab-window formation: Geology, v. 19, p. 657–660, https://doi.org/10.1130/0091-7613(1991)019<0657:RBAVAS>2.3.CO;2.

Hole, M.J., Kempton, P.D., and Millar, I.L., 1993, Trace-element and isotopic characteristics of small-degree melts of the asthenosphere: Evidence from the alkalic basalts of the Antarctic Peninsula: Chemical Geology, v. 109, p. 51–68, https://doi.org/10.1016/0009-2541(93)90061-M.

Hole, M.J., Saunders, A.D., Rogers, G., and Sykes, M.A., 1994, The relationship between alkaline magmatism, lithospheric extension and slab window formation along continental destructive plate margins, *in* Smellie, J.L., ed., Volcanism Associated with Extension at Consuming Plate Margins: Geological Society, London, Special Publication 81, p. 265–285, https://doi.org/10.1144/GSL.SP.1994.081.01.15.

Howarth, G.H., and Harris, C.J., 2017, Discriminating between pyroxenite and peridotite sources for continental flood basalts (CFB) in southern Africa using olivine chemistry: Earth and Planetary Science Letters, v. 475, p. 143–151, https://doi.org/10.1016/j.epsl.2017.07.043.

Keshav, S., Gudfinnsson, G., Sen, G., and Fei, S., 2004, High-pressure melting experiments on garnet clinopyroxenite and the alkalic to tholeiitic transition in ocean-island basalts: Earth and Planetary Science Letters, v. 223, p. 365–379, https://doi.org/10.1016/j.epsl.2004.04.029.

Kogiso, T., Hirschmann, M.M., and Frost, D.J., 2003, High-pressure partial melting of garnet pyroxenite: Possible mafic lithologies in the source of ocean island basalts: Earth and Planetary Science Letters, v. 216, p. 603–617, https://doi.org/10.1016/S0012-821X(03)00538-7.

Košler, J., Magna, T., Mlococh, B., Mixa, P., Nyvlt, D., and Holub, F.V., 2009, Combined Sr, Nd, Pb and Li isotope geochemistry of alkaline lavas from northern James Ross Island (Antarctic Peninsula) and implications for back-arc magma formation: Chemical Geology, v. 258, p. 207–218, https://doi.org/10.1016/j.chemgeo.2008.10.006.

Lambart, S., 2017, No direct contribution of recycled crust in Icelandic basalts: Geochemical Perspective Letters, v. 4, p. 7–12, https://doi.org/10.7185/geochemlet.1728.

Lambart, S., Baker, M.B., and Stopler, E.M., 2016, The role of pyroxenite in basalt genesis: Melt-PX, a melting parameterization for mantle pyroxenites between 0.9 and 5GPa: Journal of Geophysical Research, v. 121, p. 5708–5735, https://doi.org/10.1002/2015JB012762.

Le Roux, V., Dasgupta, R., and Lee, C.-T.A., 2015, Recommended mineral-melt partition coefficients for FRTEs (Cu), Ga, and Ge during mantle melting: The American Mineralogist, v. 100, p. 2533–2544, https://doi.org/10.2138/am-2015-5215.

Pertermann, M., Hirschmann, M.M., Hametner, D., Günther, D., and Schmidt, M.W., 2004, Experimental determination of trace element partitioning between garnet and silica-rich liquid during anhydrous melting: Geochemistry, Geophysics, Geosystems, v. 5, Q05A01, https://doi.org/10.1029/2003GC000638.

Putirka, K., Tao, Y., Hart, S.R., Perfitt, M.R., Jackson, M.G., and Arevalo, R., Jr., 2018, The mantle source of thermal plumes: Trace and minor elements in olivine and major oxides of primitive liquids (and why the olivine compositions don't matter): The American Mineralogist, v. 103, p. 1253–1270, https://doi.org/10.2138/am-2018-6192.

Sheldrick, T.C., Hahn, G., Ducea, M.N., Stoics, A.M., Constenius, K., and Heizler, M., 2020, Peridotite versus pyroxenite input in Mongolian Mesozoic–Cenozoic lavas, and dykes: Lithos, v. 376–377, https://doi.org/10.1016/j.lithos.2020.105747.

Søager, N., Portnyagin, M., Hoernle, K., Holm, P.M., Hauff, F., and Garbe-Schonberg, D., 2015, Olivine major and trace element compositions in southern Payenia basalts, Argentina: Evidence for pyroxenite-peridotite melt mixing in a back-arc setting: Journal of Petrology, v. 56, p. 1495–1518, https://doi.org/10.1093/petrology/egv043.

Thorkelson, D.J., and Breitsprecher, K., 2005, Partial melting of slab window margins: Genesis of adakitic and non-adakitic magmas: Lithos, v. 79, p. 25–41, https://doi.org/10.1016/j.lithos.2004.04.049.

Thorkelson, D.J., Madsen, J.K., and Sluggett, C., 2011, Mantle flow through the Northern Cordilleran slab window revealed by volcanic geochemistry: Geology, v. 39, p. 267–270, https://doi.org/10.1130/G31522.1.

Zhang, Y., Sun, C.Y.M., Huang, Z., Narantsetseg, T., Ren, Z., Li, P., and Zhang, Q., 2021, Contrasting compositions between phenocrystic and xenocrystic olivines in the Cenozoic basalts from central Mongolia: Constraints on source lithology and regional uplift: The American Mineralogist, v. 106, p. 251–264, https://doi.org/10.2138/am-2020-7431.

Printed in USA